ISSN 1027-4510, Journal of Surface Investigation: X-ray, Synchrotron and Neutron Techniques, 2023, Vol. 17, No. 3, pp. 652–655. © Pleiades Publishing, Ltd., 2023.
Russian Text © The Author(s), 2023, published in Poverkhnost', 2023, No. 6, pp. 27–31.

Polymethyl Metacrylate with a Molecular Weight of 10^7 g/mol for X-ray Lithography

V. P. Nazmov[a, b, *], A. V. Varand[a], M. A. Mikhailenko[b, **], B. G. Goldenberg[a, c], I. Yu. Prosanov[b], and K. B. Gerasimov[b]

[a] *Budker Institute of Nuclear Physics, Siberian Branch, Russian Academy of Sciences, Novosibirsk, 630090 Russia*

[b] *Institute of Solid State Chemistry and Mechanochemistry, Siberian Branch, Russian Academy of Sciences, Novosibirsk, 630090 Russia*

[c] *Collective Centre SKIF, Boreskov Institute of Catalysis, Siberian Branch, Russian Academy of Sciences, Novosibirsk, 630559 Russia*

**e-mail: V.P.Nazmov@inp.nsk.su*

***e-mail: mikhailenkoma79@gmail.com*

Received October 16, 2022; revised December 22, 2022; accepted December 22, 2022

Abstract—The paper presents the results of a study of syndiotactic polymethyl methacrylate with a molecular weight of 10^7 g/mol, synthesized by the method of ionic polymerization with radiation initiation. Changes in the chemical structure of the polymer material were analyzed by means of IR spectroscopy, differential thermal analysis, and gel permeation chromatography. The process of weight loss during thermal decomposition of the initial polymer can be divided into three stages: low-temperature, medium-temperature, and high-temperature ones. After exposure of the polymer even to minimum doses of ionizing radiation, there is no pronounced thermal effect of polymer melting. A scatter in the molecular sizes was found, as well as a relatively rapid decrease in the molecular weight under the action of X-rays in the dose range of up to 100 J/cm^3. Polydispersity at low doses is approximately 3.5 times higher than that at doses on the order of 10 kJ/cm^3. The achieved rate of latent image development was approximately five times compared with the polymer with a molecular weight of 10^6 g/mol under standard conditions. The contrast was 3.4. Microstructuring was performed by the X-ray lithography method on the VEPP-3 source with the use of synchrotron X-rays. The resulting microstructures are up to 5 μm high and about 2 μm in diameter.

Keywords: polymethyl methacrylate, IR spectroscopy, gel permeation chromatography, differential thermal analysis, contrast, X-rays, sensitivity, microstructures, X-ray lithography

DOI: 10.1134/S102745102303028X

INTRODUCTION

In X-ray lithography, the image is transferred from the X-ray mask to the X-ray sensitive layer with the use of X-rays. As the sensitive layer (resist), polymethyl methacrylate (PMMA), previously studied in the electron lithographic process [1, 2], is used due to its excellent properties like its high spatial resolution, high glass transition temperature, and high resistivity in acid-containing solutions applied in the microelectronic manufacturing [3]. The lithographic properties of PMMA were studied in detail in [4]. Under the action of X-rays, PMMA molecules undergo destruction [5, 6], which leads to reduction of the molecular weight of the polymer, which contributes to higher dissolution rate in organic solvents. The contrast of PMMA is relatively low [7, 8], but this value can be increased to 5 via optimization of the developer [9]. At a correct choice of the dose of absorbed X-rays, this fact ensures manufacturing of microstructures with almost vertical sidewalls and sidewall roughness of less than 50 nm [7].

Previous studies have shown that with increase in the molecular weight of the polymer, the ratio of the dissolution rate of the irradiated material to the dissolution rate of the unirradiated material grows at the same doses of absorbed radiation [10, 11]. On the other hand, experiments with PMMA with a molecular weight of up to 0.95×10^6 g/mol have shown the tendency of growth of the spatial resolution with increase in the molecular weight [12]. For this reason, because the synthesis of the polymer with an ultrahigh molecular weight is still insufficiently studied, reproducible results cannot be obtained, and all previous studies are limited to a polymer molecular weight of 2×10^6 g/mol.

In this work, we synthesized (the synthesis conditions will be described elsewhere) and examined the PMMA that differs from the widely used analog

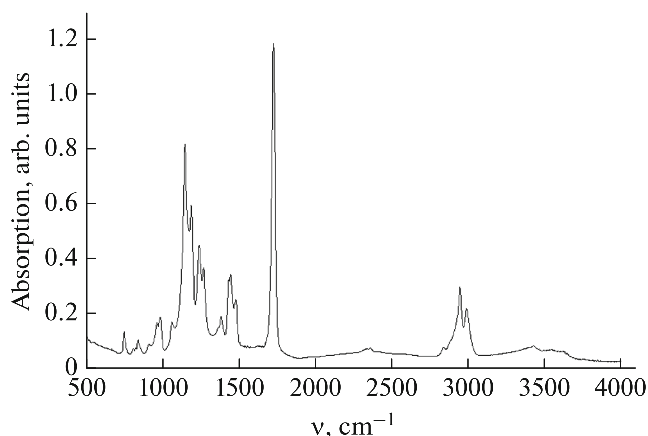

Fig. 1. IR spectrum of PMMA film 3 μm thick.

GS 233 (Evonik Industries) in the tenfold increase in the molecular weight (up to 10^7 g/mol). Basing on absorption spectra obtained in the IR range, data of differential thermal analysis, and gel permeation chromatography, we studied the changes in the material after exposure to ionizing radiation.

EXPERIMENTAL PART

First, methyl methacrylate was purified via distillation under reduced pressure with application of the IR-1M rotary evaporator (made in PRC). The polymerization was conducted in accordance with the method of radiation initiation of methyl methacrylate and subsequent heat treatment of the reaction mixture.

The IR spectra were measured with the help of the InfraLYUM FT-08 Fourier spectrometer (Lumex, Russia). For the study, films ~3–3.5 μm thick were taken, produced by pouring and subsequent drying in a vacuum oven at a temperature of 64°C for 1 h. The examination was carried out in the transmission mode in the frequency range of 4000 to 550 cm^{-1}. The spectral resolution was 4 cm^{-1}. Analysis of the spectra showed that the synthesized polymer is fully syndiotactic [13, 14] (Fig. 1).

The thermoanalytical examinations were performed in an argon flow with the use of the synchronous thermal analyzer STA 449 F/1/1 JUPITER with the mass spectrometer QMS403 CF AEOLOS (Netzsch, Germany). The heating rate was 10 K/min. The molecular-weight distribution was studied by the method of gel permeation chromatography with the help of the chromatograph with the Knauer refractometric detector (Germany), the Agilent PLgel MIXED-A column, 7.5 × 300 mm, 20 μm. The temperature was 50°C. The mobile phase was tetrahydrofuran. The flow rate was 1.5 mL/min.

The rate of dissolution of the non-irradiated PMMA was determined by two methods. First, the visible-range-light transmission of the solution was measured during dissolution of sample in GG (the solvent is described in [15]). Second, after drying of the polymer dissolved in GG with subsequent dissolution of the dried precipitate in tetrahydrofuran, the molecular weight of the former was determined by the gel permeation chromatography method. The result was approximately 15 nm/min in both cases.

Both for characterization of the properties of the polymer under study and for manufacturing of microstructures, the polymer layers were exposed to X-ray synchrotron radiation (SR) at the LIGA station [16] of the VEPP-3 source [17] in the mode optimized [18] for X-ray lithography, which corresponds to an energy of electrons in the storage ring of 1.2 GeV. For characterization of the material, layers of uniform thickness (~900 μm) were used; the variation of the dose of absorbed X-rays over the layer thickness was about 20%.

RESULTS AND DISCUSSION

Differential Thermal Analysis

The curve of mass loss during decomposition of the initial polymer can be divided into three stages: at low temperature, with the maximum decomposition rate at 260.5–261°C and the process onset at 207–209°C; at medium temperature, about 295°C; at high temperature, with the maximum decomposition rate at 379°C, the process onset at 346–348°C, and the process end at 398–400°C. With the build-up of the dose of deposited radiation, the temperature of the onset of polymer decomposition expectedly decreases from 207(209) to 152°C. Besides, lowering and broadening of the maximum of the low-temperature decomposition are observed, as well as the shift of the temperature of the end of the decomposition process towards higher temperatures of 398(400)–427(428)°C. The position of the main decomposition peak is within 376–384°C. In the curves of the differential thermal analysis, the pronounced thermal effect of polymer melting disappears after exposure even to minimum doses of deposited radiation.

Gel Permeation Chromatography

As in the case of the polymer with a molecular weight of approximately 10^6 g/mol [19], in the PMMA with a molecular weight of 10^7 g/mol, as the absorbed X-ray dose builds up, the average molecular weight decreases from 10^7 to ~ 7 × 10^4 g/mol. At the same time, decrease in the molecular weight by a factor of about 10 is observed at doses lower than in the case of GS 233 (~75 J/cm^3), which can result in higher sensitivity of the material to X-rays compared with GS 233.

It should also be noted that the polydispersity of the irradiated PMMA at low doses is as high as 8, which indicates a greater spread of the molecule weight than in the case of GS 233. However, with

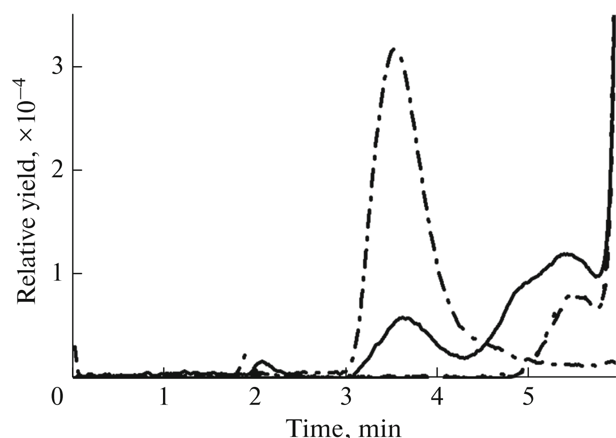

Fig. 2. Gel chromatograms of initial PMMA (dash-dotted line) and samples obtained after dissolution at 22 (solid line), 32 (dashed line), and 60°C (dotted line).

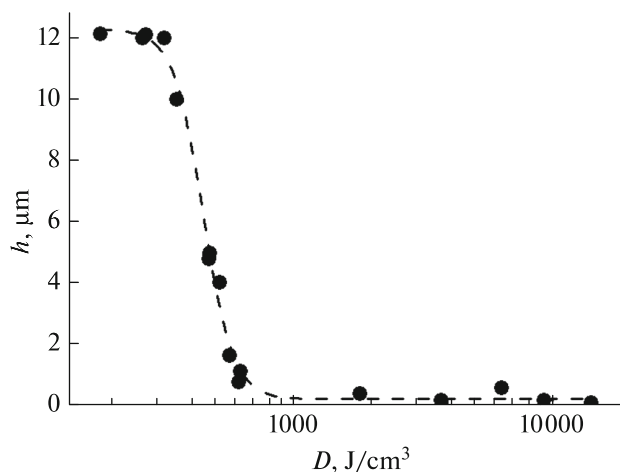

Fig. 3. Measured characteristic curve of PMMA resist with molecular weight of 10^7 g/mol.

build-up of the dose of deposited radiation to ~1 kJ/cm^3, the polydispersity decreases to the value typical of its low-molecular-weight analog (approximately 2.3), which indicates that at high doses of absorbed radiation, the degradation processes in both polymers proceed in the same way.

Contrast

During the study of the material, it turned out that the polymer dissolves poorly in the GG solution at room temperature, which manifests itself in a day in the appearance of undissolved film on the substrate surface. Dissolution of PMMA in GG is accompanied by the chemical hydrolysis reaction and formation of free carboxyl groups. This can be seen in particular in the elution process at examination by the gel permeation chromatography method (Fig. 2).

At higher dissolution temperature, the retention time grows due to the interaction of the carboxyl groups with the sorbent. The characteristic curve was therefore studied during development at 32° C by the method described in [20]. To this end, the PMMA was applied onto ceramic substrates with planar surface roughness of ~1 μm, because the adhesion of the material to substrates with small-scale surface roughness was extremely low. The experimentally obtained dependence of the thickness of the remaining resist layer on the dose of deposited radiation can be transformed into the dissolution rate and presented in the following form [4]:

$$V(D) = V_0 + \beta D^{\alpha}, \quad (1)$$

where the dose of deposited radiation is measured in kJ/cm^3 , V_0 = 15 nm/min, β = 12, and the contrast α is 3.4. The resulting characteristic curve is shown in Fig. 3. The non-zero resist thickness at doses above 800 J/cm^3 is because of the profilometer errors in the measurement of the substrate surface with relatively large scale surface roughness. As follows from the function presented in Fig. 3, a noticeable dissolution rate is observed at a dose of deposited radiation of ~300 J/cm^3, and the upper threshold is at a dose of ~600 J/cm^3. Both doses are approximately five times less than those in experiments with the PMMA with a molecular weight of 10^6 g/mol, which indicates a higher dissolution rate. A similar result of growth of the dissolution rate due to the higher temperature of the developer for the PMMA with a molecular weight of 0.95 × 10^6 g/mol was achieved in [21].

Micromanufacturing

Determination of the dependence of the dissolution rate and contrast of the synthesized high-molec-

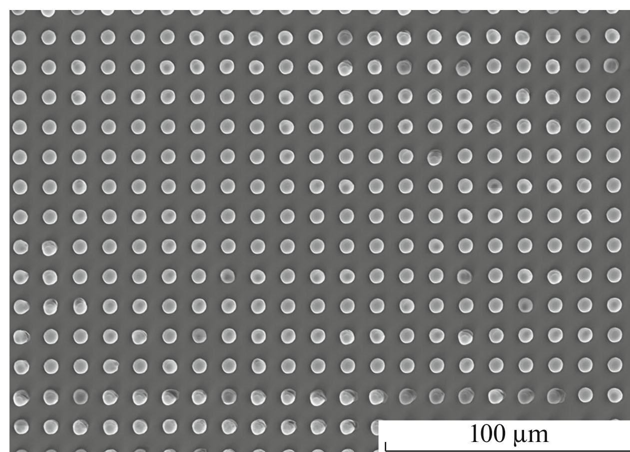

Fig. 4. Electron microscopy image of array of microstructures 4 μm high created in synthesized PMMA with molecular weight of 10^7 g/mol.

ular PMMA on the deposited dose made it possible to create microstructures on a silicon substrate by irradiation through a test X-ray mask (Fig. 4). The diameter of the microstructures was set by the topology of the gold absorber on the X-ray mask and varied in the range from 2 to 200 μm.

CONCLUSIONS

The developed high-molecular-weight PMMA with syndiotactic stereoisometry can be used for microstructuring. It features higher temperature of latent image development due to the larger size of the coil consisting of fragments of the destroyed macromolecule, which prevent the developer from penetrating.

FUNDING

The work was carried out with the equipment of the shared-use center SCSTR on the basis of the VEPP-4 – VEPP-2000 complex at BINP SB RAS, with support from the Ministry of Education and Science of the Russian Federation (project FWUS-2022-0001) regarding the study of the properties of the polymer film and under Agreement no. 075-15-2021-1359 with respect to the examination of the lithographic properties of the material and the study of the micromanufacturing process.

CONFLICT OF INTEREST

The authors declare that they have no conflicts of interest.

REFERENCES

1. I. Haller, M. Hatzakis, and R. Srinivasan, IBM J. Res. Dev. **12**, 251 (1968). https://doi.org/10.1147/rd.123.0251
2. D. L. Spears and H. I. Smith, Electron. Lett. **8**, 102 (1972). https://doi.org/10.1049/el:19720074
3. Y. Vladimirsky, O. Vladimirsky, and K. J. Morris, M. J. Klopf, G. M. Calderon, and V. Saile, Microelectron. Eng. **30**, 543 (1996). https://doi.org/10.1016/0167-9317(95)00305-3
4. J. S. Greeneich, J. Electrochem. Soc. **122**, 970 (1975).
5. Charlesby, A., *Atomic Radiation and Polymers* (Pergamon, Oxford, 1960).
6. H. Hiraoka, IBM J. Res. Dev. **21**, 121 (1977). https://doi.org/10.1147/rd.212.0121
7. F. De Carlo, D. C. Mancini, B. Lai, and J. J. Song, Microsyst. Technol. **4**, 86 (1998). https://doi.org/10.1007/s005420050102
8. V. P. Nazmov, L. A. Mezentseva, V. F. Pindyurin, V. V. Petrov, E. N. Yakovleva, Nucl. Instrum. Methods Phys. Res., Sect. A **448**, 493 (2000). https://doi.org/10.1016/S0168-9002(00)00238-2
9. F. J. Pantenburg, S. Achenbach, and J. Mohr, J. Vac. Sci. Technol., B **16**, 3547 (1998). https://doi.org/10.1116/1.590494
10. Moreau, W.M., *Semiconductor Lithography: Principles, Practices, and Materials* (Plenum, New York, 1988).
11. M. Yan, S. Choi, K. R. V. Subramanian, and I. Adesida, J. Vac. Sci. Technol., B **26**, 2306 (2008). https://doi.org/1.0.1116/1.3002562
12. M. Khoury and D. K. Ferry, J. Vac. Sci. Technol. V **14** (1), 75 (1996). https://doi.org/10.1116/1.588437
13. H. Nagai, J. Appl. Polym. Sci. **7**, 1697 (1963). https://doi.org/10.1002/app.1963.070070512
14. H. A. Willis, V. J. I. Zichy, and P. J. Hendra, Polymer **10**, 737 (1969). https://doi.org/10.1016/0032-3861(69)90101-3
15. W. Glashauser and G.-V. Ghica, FRG Patent No. 039110 (1980).
16. B. G. Goldenberg, A. G. Lemzyakov, V. P. Nazmov, and V. F. Pindyurin, Phys. Procedia **84**, 205 (2016). https://doi.org/10.1016/j.phpro.2016.11.036
17. P. A. Piminov, G. N. Baranov, A. V. Bogomyagkov, D. E. Berkaev, V. M. Borin, V. L. Dorokhov, S. E. Karnaev, V. A. Kiselev, E. B. Levichev, O. I. Meshkov, S. I. Mishnev, S. A. Nikitin, I. B. Nikolaev, S. V. Sinyatkin, P. D. Vobly, K. V. Zolotarev, and A. N. Zhuravlev, Phys. Procedia **84**, 19 (2016). https://doi.org/10.1016/j.phpro.2016.11.005
18. V. Nazmov, B. Goldenberg, A. Vasiliev, and V. Asadchikov, J. Micromech. Microeng. **31**, 055011 (2021). https://doi.org/10.1088/1361-6439/abf331
19. A. El-Kholi, J. Mohr, and V. Nazmov, Nucl. Instrum. Methods Phys. Res., Sect. A **448**, 497 (2000). https://doi.org/10.1016/S0168-9002(00)00239-4
20. D. Kunka, J. Mohr, V. Nazmov, J. Meiser, P. Meyer, M. Amberger, F. Koch, J. Schulz, M. Walter, T. Duttenhofer, A. Voigt, G. Ahrens, and G. Grutzner, Microsyst. Technol. **20**, 2023 (2014). https://doi.org/10.1007/s00542-013-2055-x
21. S. McNamara, J. Micromech. Microeng. **21**, 015002 (2011). https://doi.org/10.1088/0960-1317/21/1/015002